

Supporting Information

Structure engineering of alveoli-like ZSM-5 with encapsulated Pt nanoparticles for the enhanced benzene oxidation

Jian Tian,^a Lixue Qi,^a Quan Zhang,^a Guowu Zhan,^b Daohua Sun^{a*} and Qingbiao Li

^{a, c}

^a Department of Chemical and Biochemical Engineering, College of Chemistry and Chemical Engineering, Xiamen University, Xiamen 361005, PR China

^b College of Chemical Engineering, Huaqiao University, Xiamen, Fujian 361021, P. R. China

^c College of Food and Biological Engineering, Jimei University, Xiamen 361021, PR China

Corresponding Author:

*Daohua Sun. E-mail address: sdaohua@xmu.edu.cn

EXPERIMENTAL

Catalyst characterization

Scanning electron microscopy (SEM, ZEISS SIGMA, Germany) was employed to observe the size and morphology of samples. Transmission electron microscopy (TEM), high-resolution transmission electron microscopy (HRTEM), and corresponding energy dispersive X-ray spectroscopy (EDS) elemental mapping images were obtained on TECNAI F30, USA. X-ray diffraction (XRD) spectra of the catalysts were obtained on an automated X-ray diffractometer (Rigaku Ultima IV, Japan) over the 2θ range of $5^\circ - 90^\circ$. X-ray photoelectron spectra (XPS) were recorded using a Quantum 2000 instrument. X-ray fluorescence analysis (XRF) was conducted on ARL Quant'X (Thermo Fisher Scientific, USA) in vacuum. All peaks were normalized by using the $1s$ peak as the reference peak. The coordination chemistry and speciation of Si of samples were determined by ^{29}Si nuclear magnetic resonance spectroscopy (^{29}Si NMR, AVANCE III 400 MHz, Bruker). The functional groups of samples were characterized by diffuse reflectance infrared Fourier transform spectroscopy (DRIFTS), which was performed using an FTIR spectrometer (Thermo, Nicolet iS50). The elemental compositions of the as-obtained samples were determined using the inductively coupled plasma ((ICP, PerkinElmer ICP 2100).

Surface areas of the samples were analyzed using the BET (Brunauer-Emmett-Teller) method via N_2 adsorption. The mesopore and micropore size distribution profiles were recorded by the Barrett-Joyner-Halenda (BJH) model on a

Micromeritics ASAP 2020 analyzer. All of the samples were degassed at 200 °C for 2 h under vacuum prior to measurement.

Temperature-programmed desorption of ammonia (TPD-NH₃) was measured on Micromeritics Auto Chem II 2920 instrument analyzer equipped with a quartz reactor and a thermal conductivity detector (TCD). Before the test, the 0.05 g sample was pretreated at 300°C and 30 mL/min argon flow rate for 1 h, with a heating rate of 5°C/min. After the sample was cooled to 50 °C, ammonia was adsorbed from a 10 %NH₃+N₂ (balance) flow at 50 °C for 60 min. TPD curve was recorded in a He flow (40 mL/ min) in the range from 30 °C to 700 °C.

In situ DRIFTS spectra were performed on a Nicolet 6700 (Thermo Nicolet) FT-IR spectrometer over the range of 1800 and 2300 cm⁻¹ with a liquid-nitrogen-cooled MCT detector. First, the catalyst was loaded to a high-temperature IR cell, a N₂ flow (30 mL/min) was passed through the IR cell at 200 °C for 30 min to evacuate any adsorbed unwanted species and then left to cool to room temperature. The background spectrum was first obtained in N₂ and subtracted from the acquired sample spectrum. Subsequently, the CO of 40 mL/min was introduced for 30 minutes at room temperature, and the in-situ DRIFTS spectra were recorded when the CO was desorbed.

Enrichment efficacy Evaluation

Benzene enrichment performance of the catalysts were probed using a fixed-bed reactor (0.01 m). Approximately 50 mg samples were putted into the fixed-bed reactor

and passed through the N₂ flow (30 mL/min) at 200 °C for 30 min to evacuate the adsorbed species. The hourly space velocity (SV) was varied 20 000 mL/(g h), and the concentration of benzene was 1000 ppm. The benzene outlet concentration was measured at 25 °C and 180 °C, respectively, along with a gas chromatographic system equipped with both thermal conductivity detector and flame-ionization detector.

Finite-Element Simulation Methods.

The finite-element analysis (FEA) was conducted using COMSOL Multiphysics. To reduce the computational cost, the numerical simulation was implemented in a 2D mode. The model of ZSM-5 was set up as a circular solid with a diameter size of 400 nm, which served as the calculated domain. The model of alveoli-like ZSM-5 was plotted as a middle spherical shell (radius of 240 nm and thickness of 30 nm), which is connected with little spherical shell (radius of 30 nm and thickness of 5 nm). This model could effectively simplify the structure of alveoli-like ZSM-5 while maintaining the mass transfer ability of mesopores. The “Transport of Diluted Species” module was used to solve the mass transport of the benzene. The diffusion constants of ZSM-5 and alveoli-like ZSM-5 were taken from the Fick’s second law. The benzene of 1000 ppm was introduced to the boundary of the two modules to calculate the concentration distribution of benzene over the model. All the boundary was set to be an inlet with an inflow velocity of 3.53 m s⁻¹ to model the flow. The flow field was solved by the following equation.

$$\frac{\partial C_i \cdot \varepsilon_p}{\partial t} + \nabla \cdot (-D_i \cdot \nabla C_i) + u \cdot \nabla C_i = R_i$$

where C_i is the concentration, t is the time, ε_p is the porosity, D_i is the diffusion coefficient and u is the velocity.

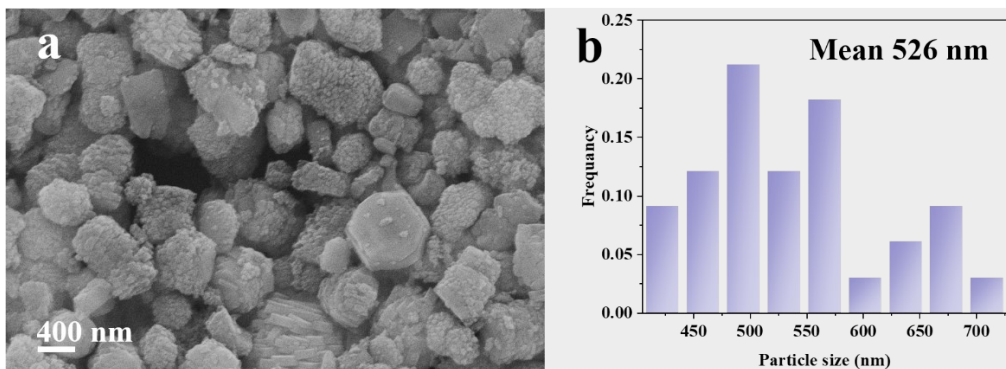


Figure S1. (a) TEM of Pt/PZ5 and (b) corresponding particle size distribution. The particle size distribution was obtained from TEM images by measuring at least 50 particles.

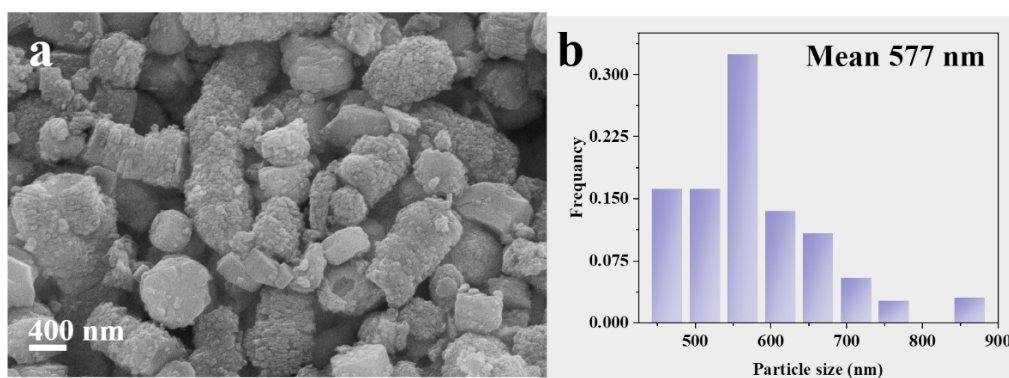


Figure S2. (a) TEM of Pt/PZ5 (24 h) and (b) corresponding particle size distribution.

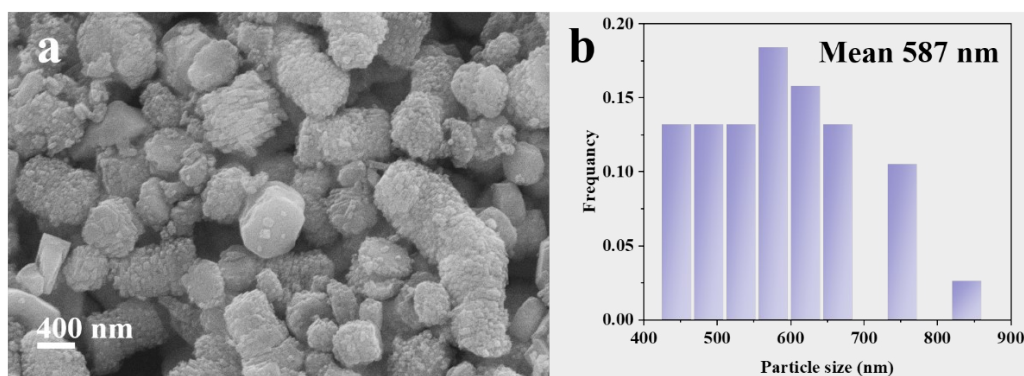


Figure S3. (a) TEM of Pt@PZ5 (48 h) and (b) corresponding particle size distribution.

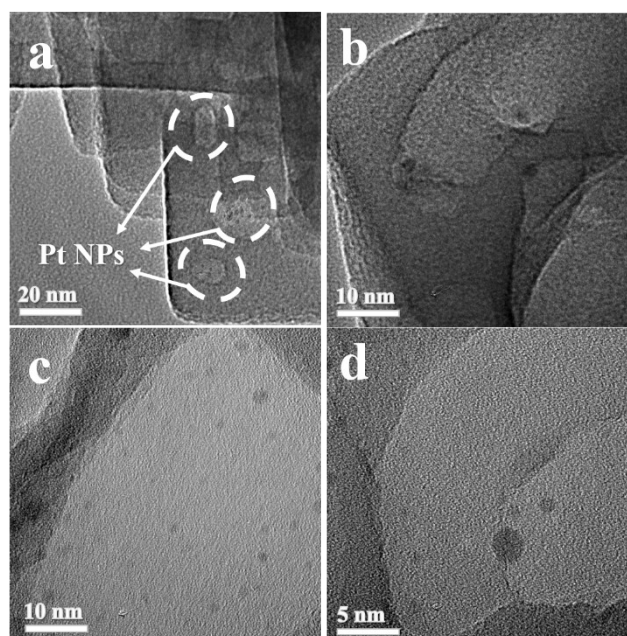


Figure S4. TEM images of alveoli-like Pt@PZ5 at a higher magnification

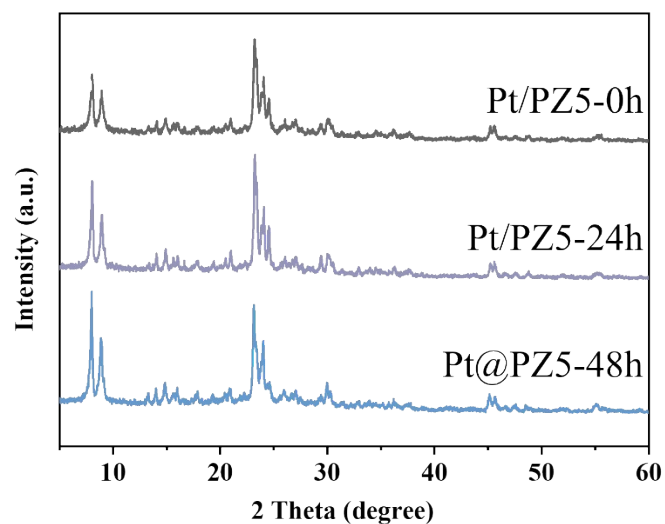


Figure S5. XRD patterns of Pt/PZ5 (0 h), Pt/PZ5 (24 h) and the alveoli-like Pt@PZ5 (48 h)

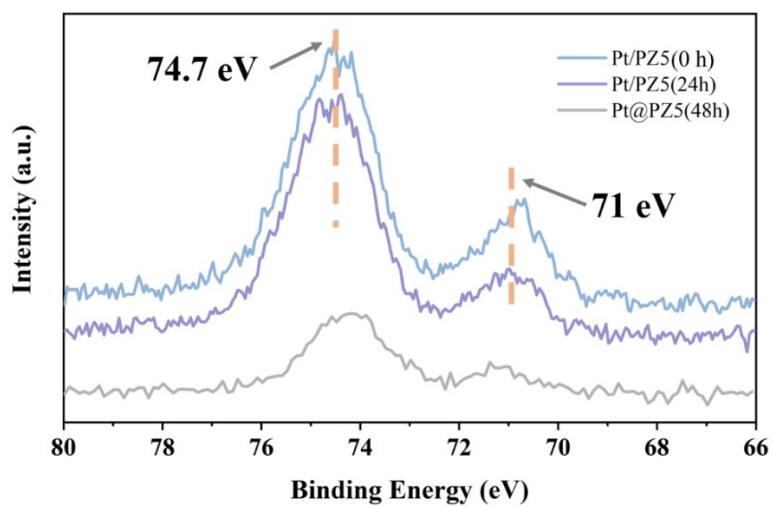


Figure S6. XPS spectra of Pt 4f over Pt/PZ5 (0 h), Pt/PZ5 (24 h) and the alveoli-like Pt@PZ5 (48 h)

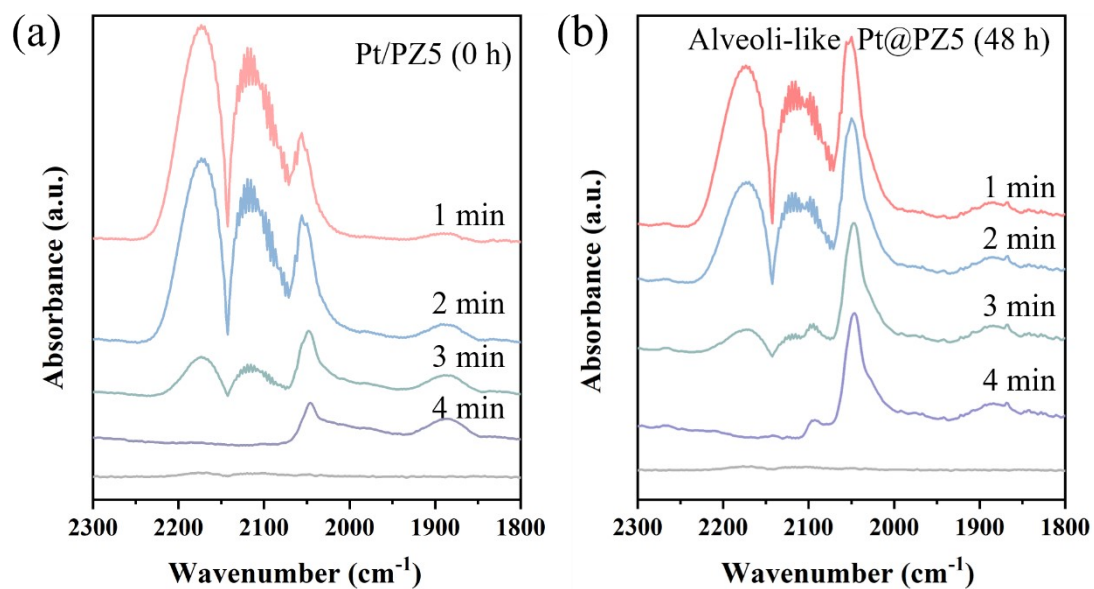


Figure S7. In situ CO-DRIFTS of (a) Pt/PZ5 (0 h) and (b) alveoli-like Pt@PZ5 (48 h)

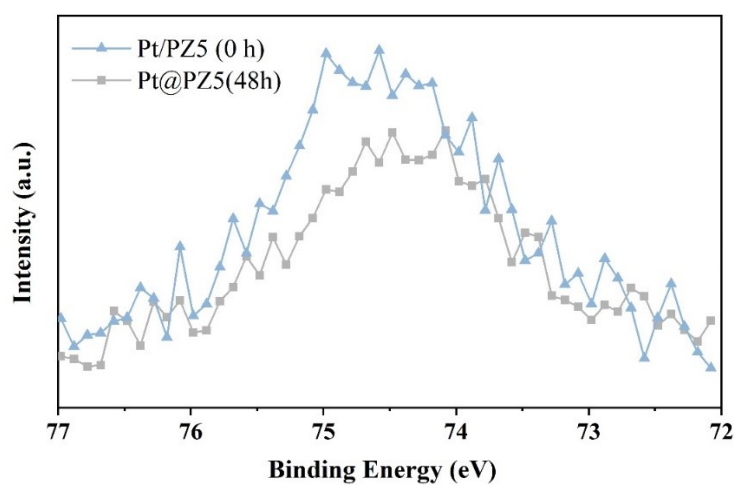


Figure S8. XPS spectra of Al over Pt/PZ5 (0 h) and Pt@PZ5 (48)

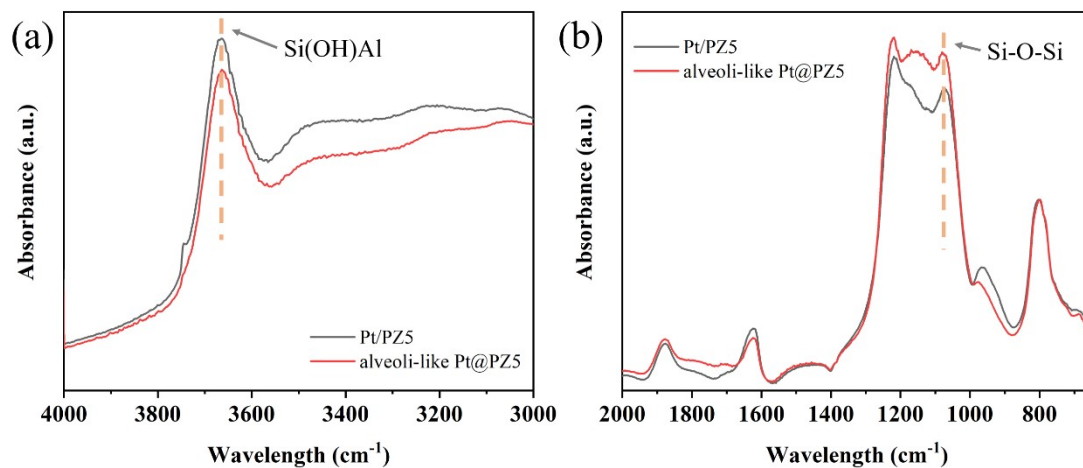


Figure S9. DRIFTS spectra of (a) Pt/PZ5 (0 h) and (b) alveoli-like Pt@PZ5 (48 h)

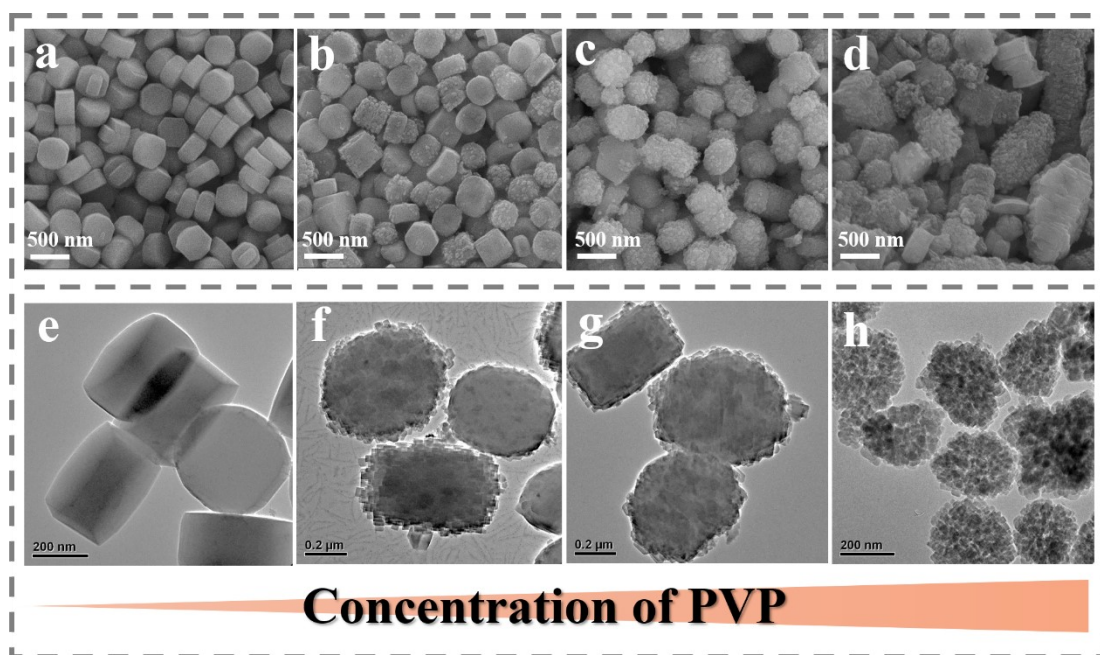


Figure S10. SEM and TEM images of (a, e) Pt/ZSM-5, (b, f) Pt/PZ5-1, (c, g) Pt/PZ5-2, and (d, h) Pt/PZ5-3

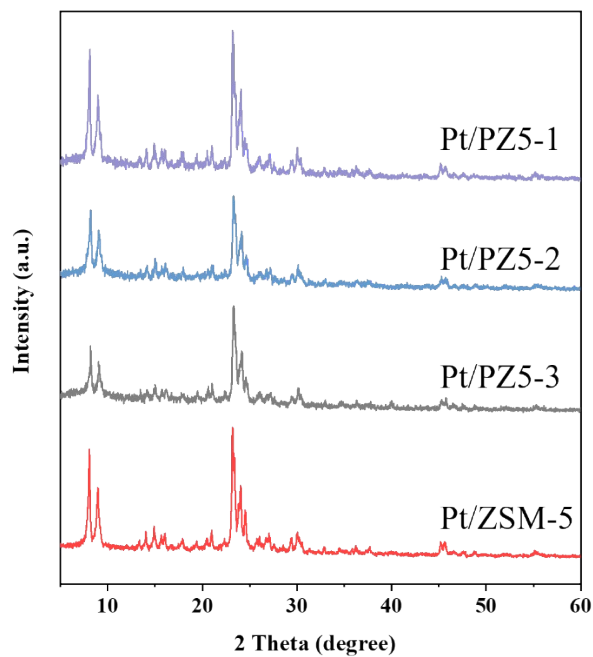


Figure S11. XRD patterns of Pt/ZSM-5, Pt/PZ5-1, Pt/PZ5-2, and Pt/PZ5-3

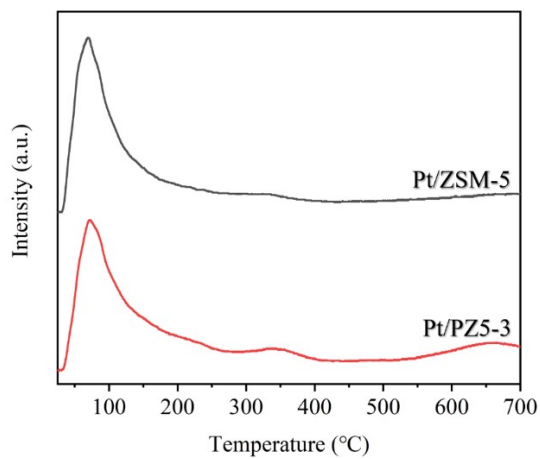


Figure S12. NH₃-TPD profiles of Pt/ZSM-5 and Pt/PZ5-3

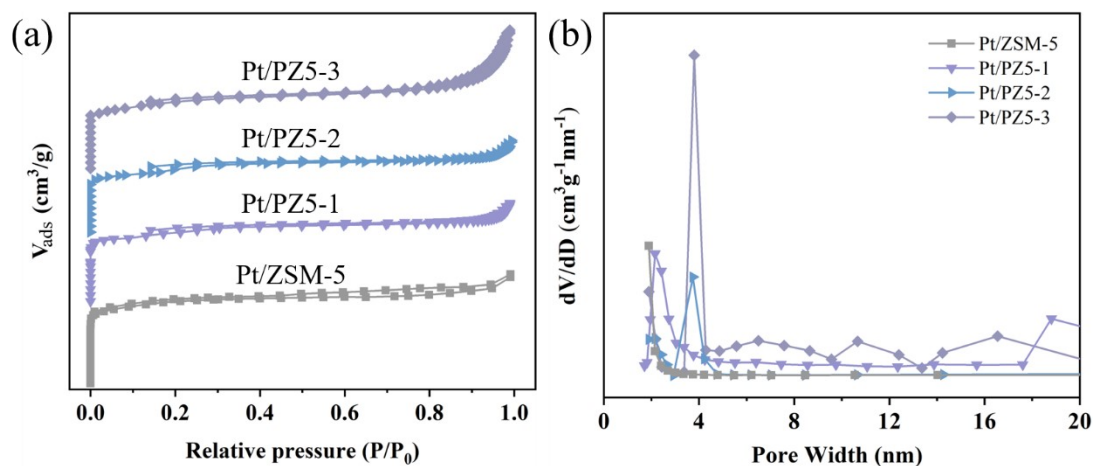


Figure S13. (a) N_2 adsorption-desorption isotherms and (b) corresponding mesopore size distributions from the BJH model

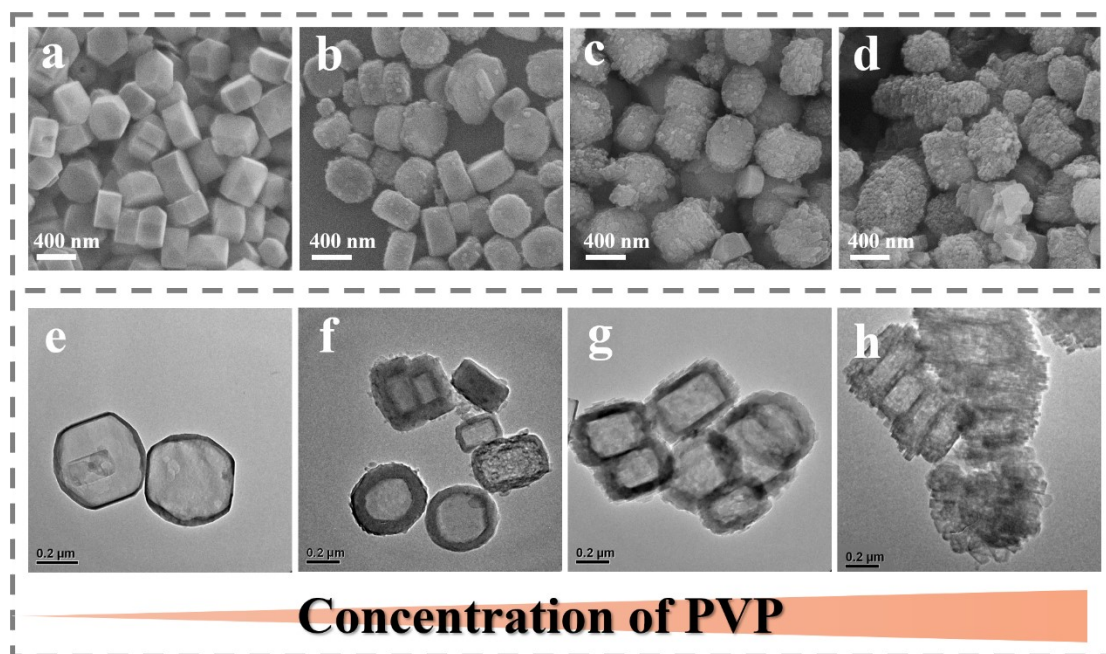


Figure S14. SEM and TEM images of (a, e) Pt@ZSM-5, (b, f) Pt@PZ5-1, (c, g) Pt@PZ5-2, and (d, h) Pt@PZ5-3

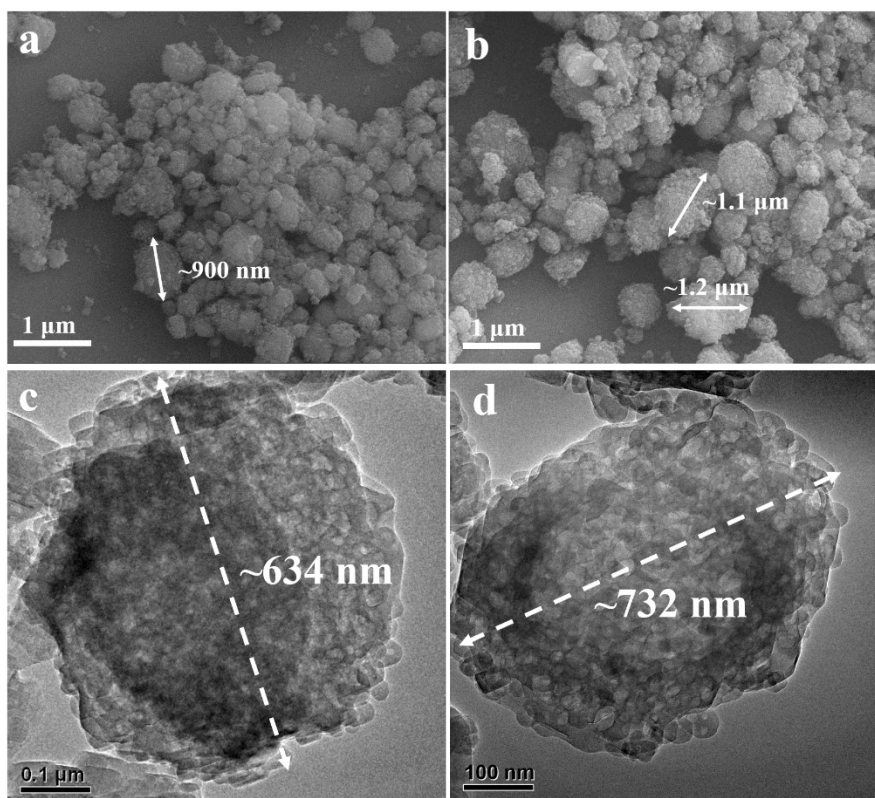


Figure S15. SEM and TEM images of (a, c) alveoli-like Pt@PZ5 (~2 wt%) and (b, d) alveoli-like Pt@PZ5 (~2.4 wt%)

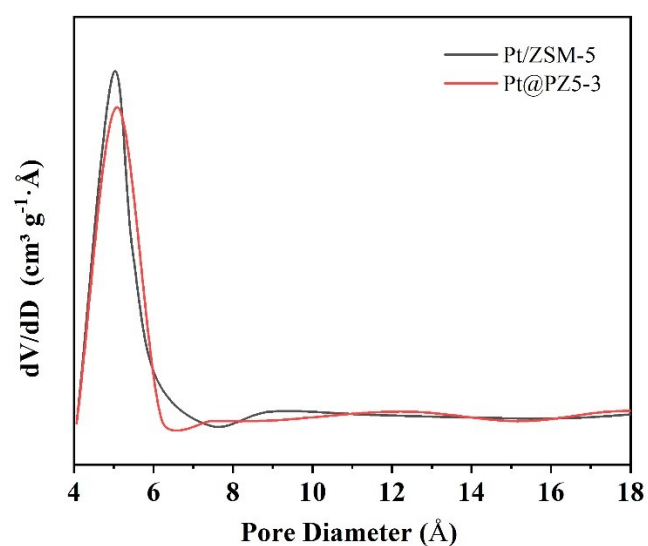


Figure S16. Pore size distribution of micropores.

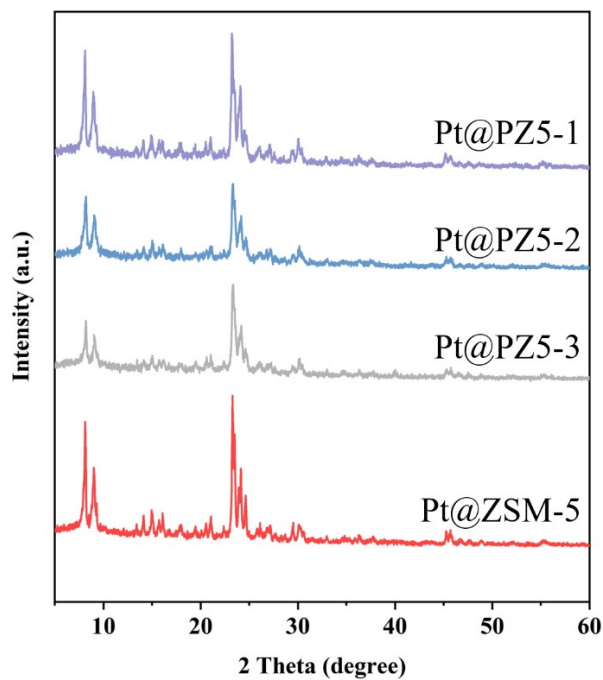


Figure S17. XRD patterns of Pt@ZSM-5, Pt@PZ5-1, Pt@PZ5-2, and Pt@PZ5-3

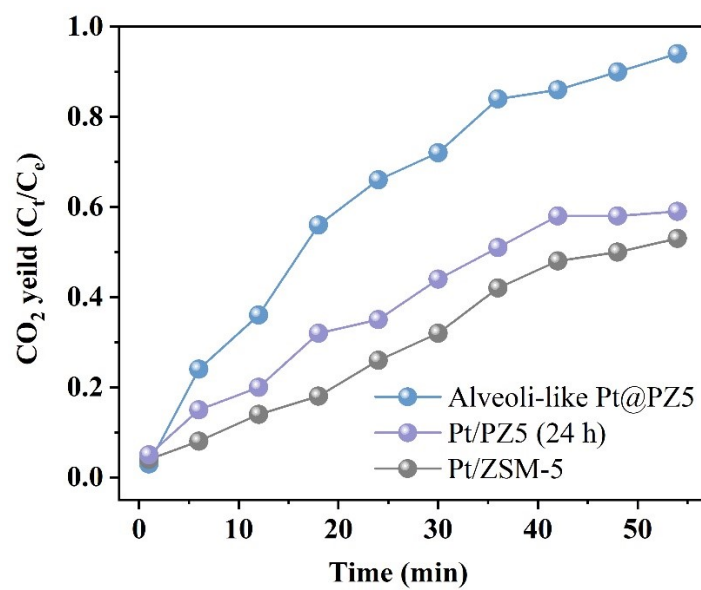


Figure S18. CO₂ yields over the prepared catalysts

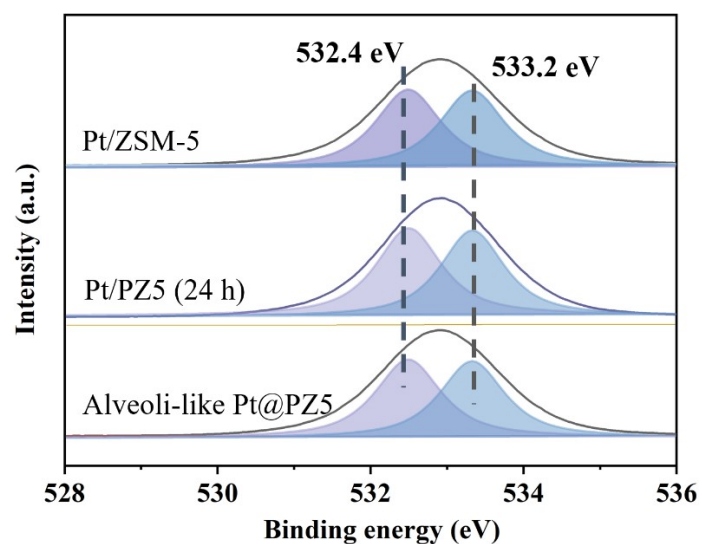


Figure S19. XPS spectra of O 1s over Pt/ZSM-5, Pt/PZ5 (24 h) and alveoli-like

Pt@PZ5

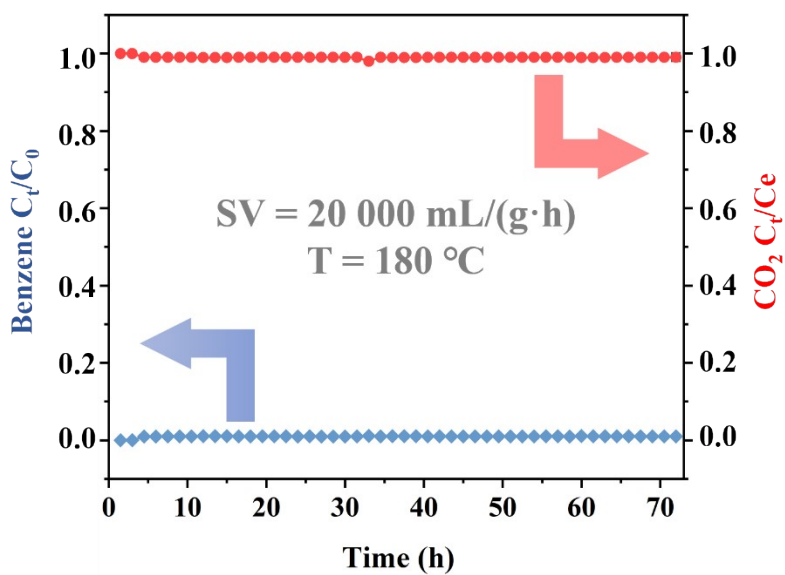


Figure S20. Benzene removal efficiency and CO₂ yield over alveoli-like Pt@PZ5 as a

function of onstream reaction time

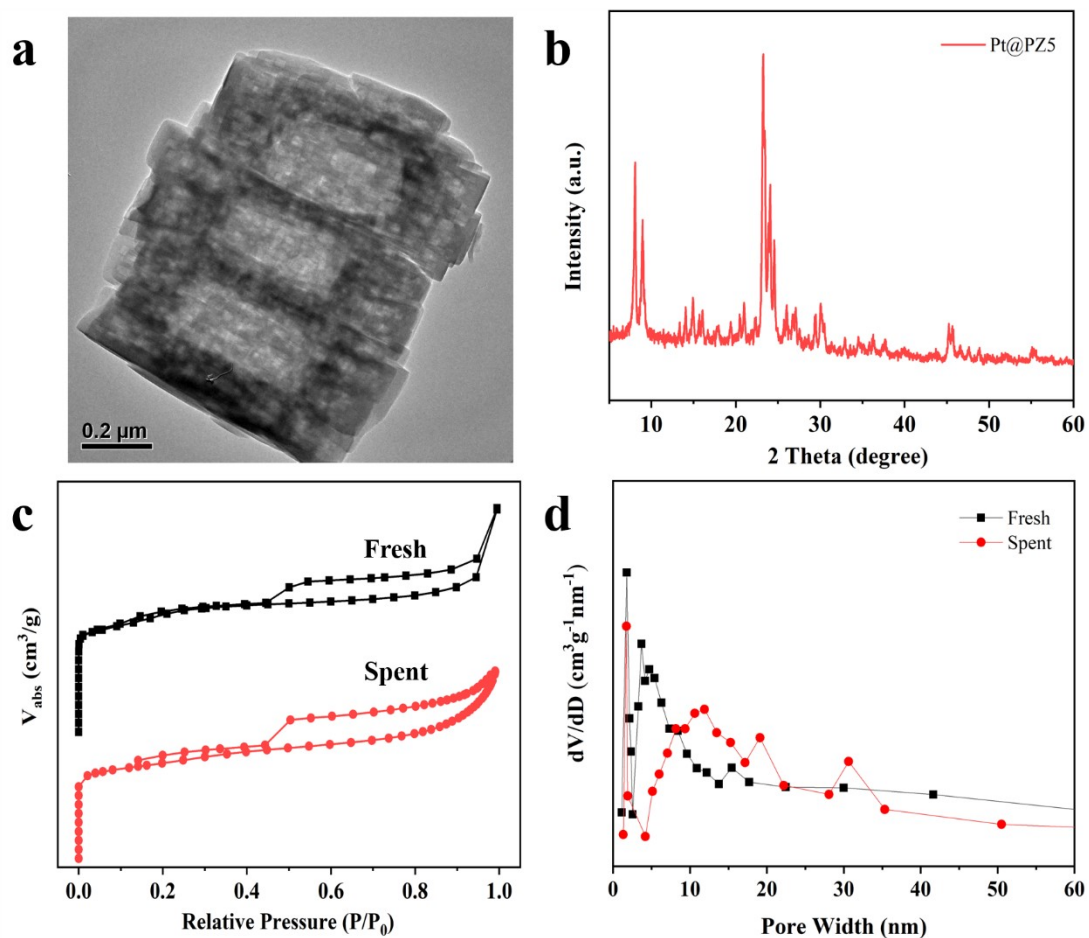


Figure S21. (a) TEM (b) XRD patterns (c) N₂ adsorption-desorption isotherms and (d) pore size distribution over the spent catalysts

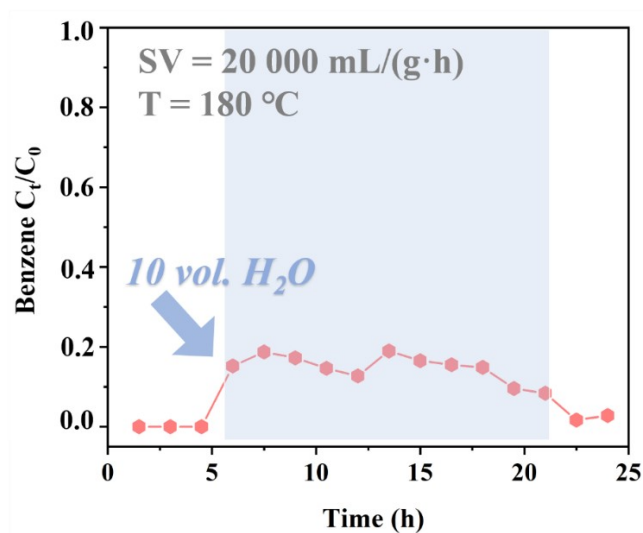


Figure S22. Benzene removal efficiency over alveoli-like Pt@PZ5 in the presence of 10 vol. % water vapors

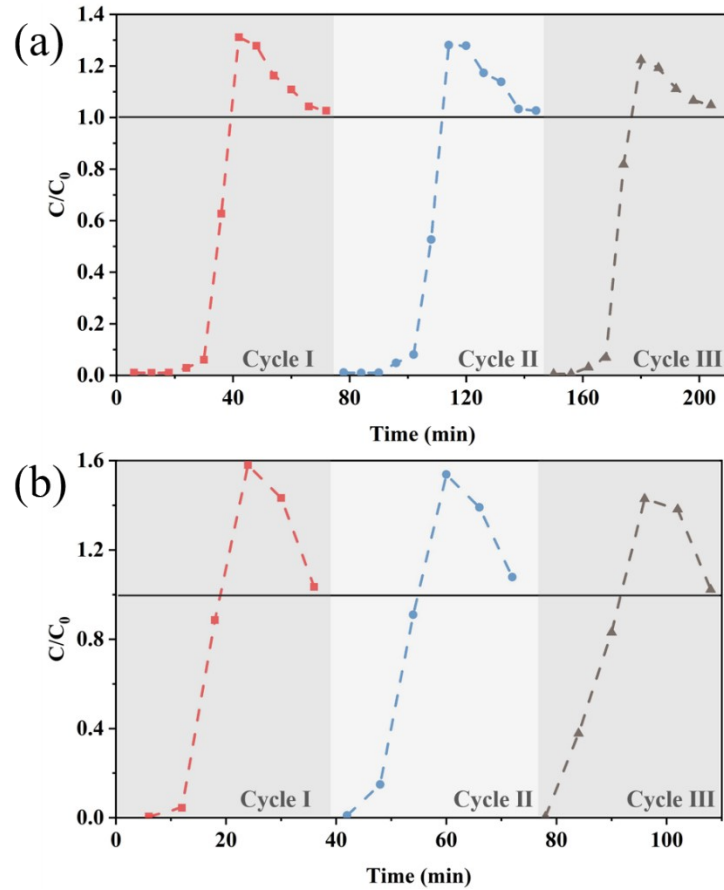


Figure S23. Cycle breakthrough curve of benzene as a function of time over (a) ZSM-5 and (b) alveoli-like PZ5: $m = 50$ mg, $T = 180$ °C, $SV = 20\ 000$ mL/(g·h)

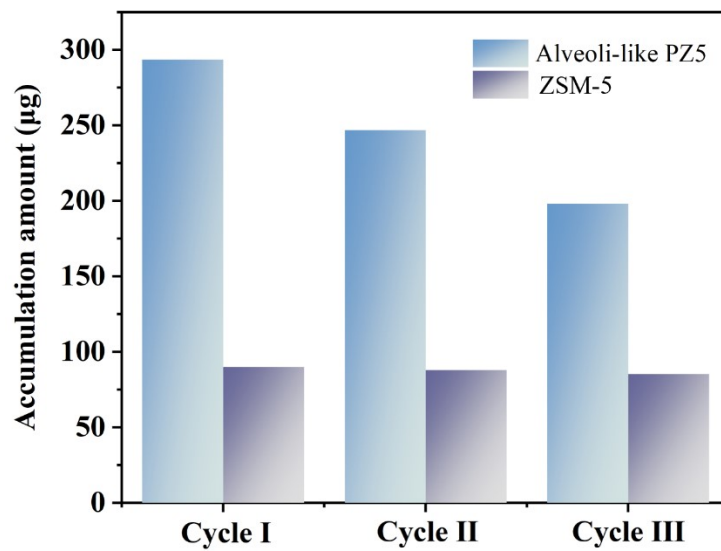


Figure S24. Data showing the amount of benzene in the ZSM-5 and alveoli-like PZ5 during the cycle adsorption-desorption process

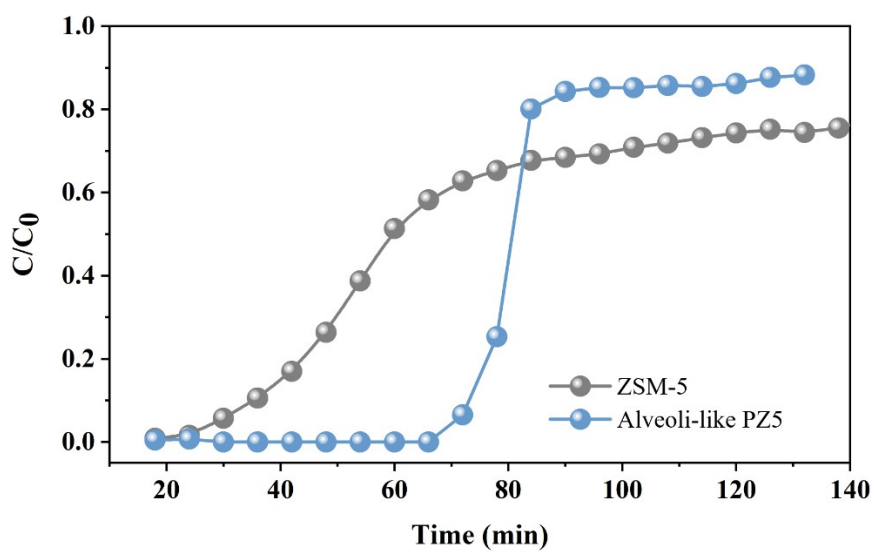


Figure S25. Breakthrough curve of benzene as a function of time over ZSM-5 and alveoli-like PZ5: $m = 50$ mg, $T = 25$ °C, $SV = 20\ 000$ mL/(g·h)

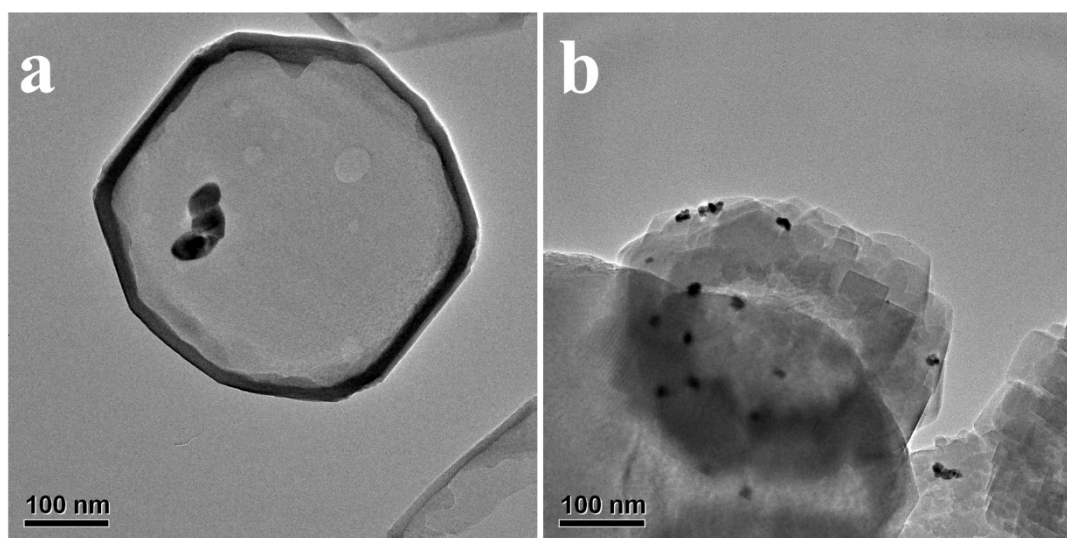


Figure S26. TEM of (a) Pt@ZSM-5 and (b) Pt/PZ5 (24 h) after calcination at 850 °C for 360 min

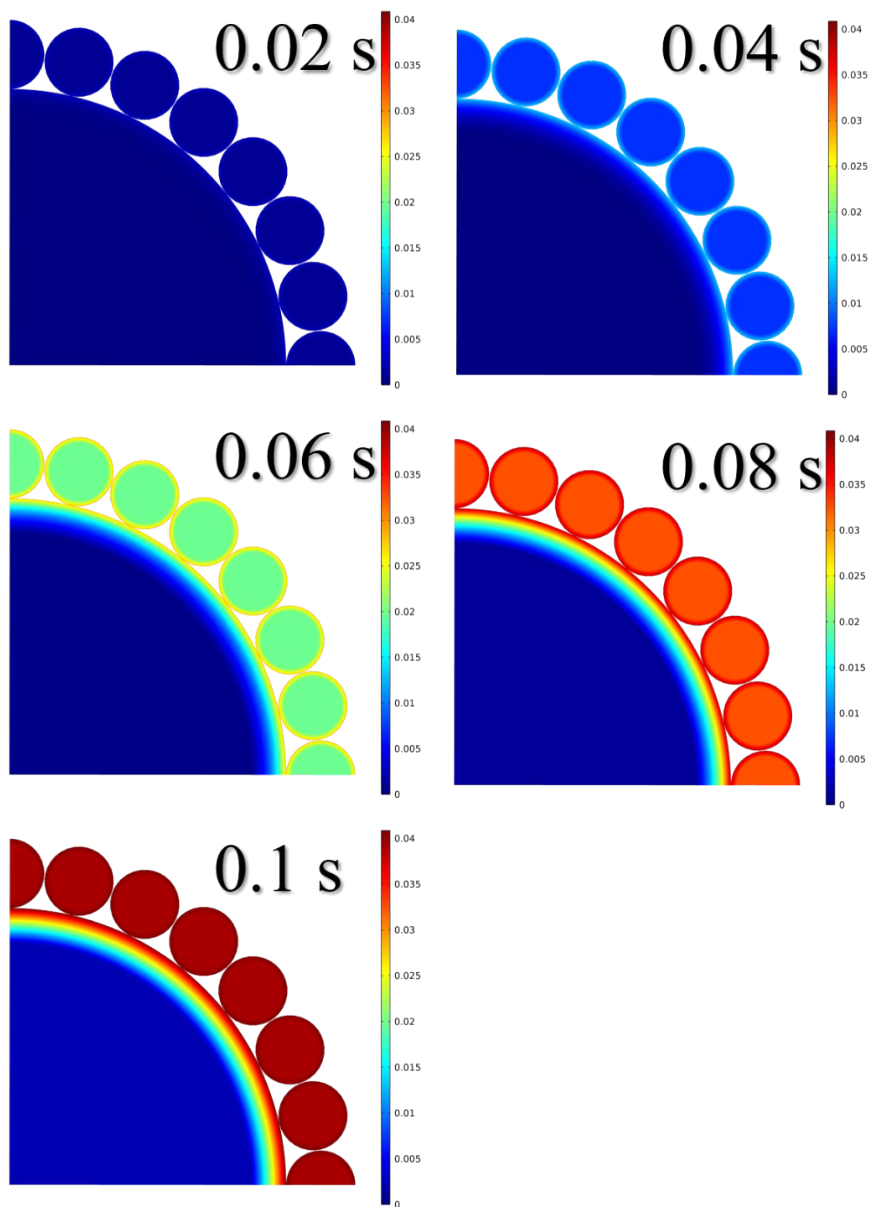


Figure S27. Computed concentration and distribution of benzene on alveoli-like PZ5

as a function of diffusion time

Table S1. Structural characteristics and properties

Parameter	Surface area (m ² /g) ^a	Micropore volume (cm ³ /g) ^a	Pore volume (cm ³ /g) ^a	Average pore size (nm) ^a
Pt/ZSM-5	403	0.10	0.36	2.26
Pt/PZ5-1	311	0.09	0.42	3.65
Pt/PZ5-2	321	0.12	0.37	3.13
Pt/PZ5-3	407	0.10	0.36	2.61
Hollow Pt@ZSM-5	366	0.09	0.65	3.78
Pt@PZ5-1	369	0.09	0.46	3.51
Pt@PZ5-2	347	0.13	0.45	3.97
Pt@PZ5-3	405	0.12	0.47	4.65

^aBET method